Energy Conversion and Management 76 (2013) 253–259

Contents lists available at ScienceDirect

Energy Conversion and Management

journal homepage: www.elsevier.com/locate/enconman

Novel neural-analytical method for determining silicon/plastic solar cells and modules characteristics

Hassan Fathabadi *

Engineering Department, Kharazmi University, Tehran, Iran

ARTICLE INFO

Article history:
Received 10 April 2013
Accepted 24 July 2013

Keywords:
Solar cell characteristics
Neural network
Parameters extraction
Lambert *W* function

ABSTRACT

In this paper, a novel method is proposed to determine the characteristics of silicon solar cell, module and plastic solar cell. Feed-forward artificial neural network together with Lambert *W* function are used to determine the characteristics. The current–voltage (*I*–*V*) and power–voltage (*P*–*V*) curves of silicon/plastic solar cells and module are determined. Five model parameters of the solar cell and module are calculated using the proposed technique which compares the Lambert *W* function representation of the current–voltage characteristic with the learned feed-forward neural network model of the current–voltage relation. Simulation results show a very good agreement between the calculated characteristic curves and experimental data. Also errors are calculated to evaluate the accuracy of the proposed method. The accuracy of the proposed method is compared with other related methods to validate the superiority of the proposed method. As will be shown, the novel contributions of the proposed method can be summarized as: firstly, the proposed method has the accuracy which is much better than other methods and secondly, the current and power errors in the proposed method are generally very lower than these errors in other methods even at the Maximum Power Point (MPP).

1. Introduction

Using photovoltaic phenomena to generate electrical energy has attracted many researchers because of its benefits in economical and environmental considerations. Consequently, solar cells and solar power generation are the topics which are addressed by many research projects. An appropriate model of a solar cell and the determination of its parameters are basic subjects in solar power generation. Since 1980, several models have been developed for modeling the non-linear characteristics of solar cells such as (*I*–*V*) and (*P*–*V*) curves. The electrical equivalent circuit based on the Shockley diode equation is the traditional model to describe a solar cell. The single diode model, which has been presented in many previously published works, is the basic equivalent circuit [1–7]. This model consists of five parameters, which are called ideality factor (n), series resistance (R_s), shunt resistance (R_p), photocurrent (I_L) and saturation current (I_o). Exponential nonlinearity of the current equation in the single diode model causes many difficulties in exact extraction of these five parameters [8]. Over the years, several parameters extraction methods have been developed. One usual method is numerical method that a polynomial is used to demonstrate the current–voltage relationship of the solar cell and furthermore iterative schemes such as the recursive least-squares method [8] and Newton–Raphson method [9] are applied to calculate all the model parameters. The convergency rates in these schemes strictly depend to the initial values used in the recursive technique and even there is not any guarantee for convergency of these methods. Another method is analytic method [10] which was presented to express the transcendental current–voltage characteristic containing parasitic power consuming parameters such as resistances. A very important tool to solve the transcendental equations is Lambert W function [8–14]. Some physical applications of Lambert W function can be found in [15,16]. To days, finding analytical solutions for determining the five parameters of the single diode model of the solar cell is an interesting research. Recently, various high accuracy techniques have been presented, such as genetic algorithm [17], pattern search [18], particle swarm optimization [19], semi-analytic method [20], semi-pattern search [21], differential evolution [22] and combination of analytic method and Lambert W function [23–26]. Based on the solar cell model, a genetic algorithm was also used for characterizing a photovoltaic panel and optimizing its parameters [27].

In this paper, by considering the advantages of other numerical and analytic methods, a novel neural-analytical technique, which is based on the application of feed-forward artificial neural network together with Lambert *W* function, is proposed to determine the characteristics of solar cells and modules. To validate the supe-

* Current address: National Technical University of Athens, Greece. Tel./fax: +98 21 88884321.

E-mail addresses: h4477@hotmail.com, h.fathabadi@khu.ac.ir

0196-8904/$ - see front matter © 2013 Elsevier Ltd. All rights reserved.
http://dx.doi.org/10.1016/j.enconman.2013.07.055

Nomenclature

LMS	least mean square
CMAE	maximum absolute current error (A)
CMAEmp	maximum absolute current error at the maximum power point (A)
G_p	conductance of the shunt resistance (Ω^{-1})
R_p	shunt resistance of the cell (Ω)
I	output current of the cell (A)
I_L	photocurrent (A)
I_{mp}	current at the maximum power point (A)
I_{sc}	short circuit current (A)
I_o	saturation current of the equivalent diode (A)
K	Boltzmann constant (1.38×10^{-23} J/K)
n	ideality factor of the cell
N	number of measurements
R_s	series resistance of the cell (Ω)
T	cell temperature (K)
PMAE	maximum absolute power error (W)
PMAE$_{mp}$	maximum absolute power error at the maximum power point (W)
q	electron charge (1.6×10^{-19} °C)
$V_T = \frac{KT}{q}$	thermal voltage of the solar cell
V	output voltage of the cell (V)
V_{ci}	computed values of the I–V curves for a given voltage point
V_{ei}	experimental values of the I–V curves for a given voltage point
V_{mp}	voltage at the maximum power point (V)
V_{oc}	open circuit voltage (V)

riority and accuracy of the proposed method, the comparative simulation results carried out in Matlab/Simulink environment are presented. Experimental and simulation results explicitly will validate the superiority of the proposed method in comparison with other methods.

2. Theory of analytical solutions

The I–V characteristic of a solar cell using the single diode model can be expressed as

$$I = I_L - \frac{V + IR_s}{R_p} - I_o\left[\exp\left(\frac{V + IR_s}{nV_T}\right) - 1\right] \quad (1)$$

By solving Eq. (1) using Lambert W function, the output current and voltage of the solar cell can be found as following [10]:

$$I(V) = \frac{R_p(I_L + I_o) - V}{R_s + R_p} - \frac{nV_T}{R_s} \cdot W\left\{\frac{R_sR_pI_o}{nV_T(R_s + R_p)}\exp\left[\frac{R_p(R_sI_L + R_sI_o + V)}{nV_T(R_s + R_p)}\right]\right\} \quad (2)$$

and

$$V(I) = R_p(I_L + I_o - I) - R_sI - nV_T \cdot W\left\{\frac{R_pI_o}{nV_T}\exp\left(\frac{R_p(I_L + I_o - I)}{nV_T}\right)\right\} \quad (3)$$

By multiplying the right and left sides of Eq. (2) by V, the output power can be earned as

$$P(V) = V \cdot I(V) = \frac{R_p(I_L + I_o)V - V^2}{R_s + R_p} - \frac{nVV_T}{R_s} \cdot W\left\{\frac{R_sR_pI_o}{nV_T(R_s + R_p)}\exp\left[\frac{R_p(R_sI_L + R_sI_o + V)}{nV_T(R_s + R_p)}\right]\right\} \quad (4)$$

From Eq. (3), the integration of the cell voltage $V(I)$ can be calculated as following [23]:

$$S(V, I) = \int_0^I V(I)dI = \frac{1}{2A}\left[(-V - BI + C)^2 - (-V + C)^2\right] - \frac{1}{2}BI^2 + ADI \quad (5)$$

Comparing Eq. (5) with the integration of Eq. (3) results that

$$A = R_p \quad (6)$$

$$B = R_s + R_p \quad (7)$$

$$C = nV_T + R_p(I_L + I_o) \quad (8)$$

$$D = I_L + I_o \quad (9)$$

Using Eqs. (6)–(8), three parameters can be obtained as

$$G_p = \frac{1}{R_p} = \frac{1}{A} \quad (10)$$

$$R_s = B - A \quad (11)$$

$$n = \frac{C - AD}{V_T} \quad (12)$$

By replacing Eqs. (10)–(12) in Eq. (1), the fourth parameter (I_o) can be expressed as

$$I_o = \frac{D - I - \frac{V + I(B-A)}{A}}{\exp\left[\frac{V + I(B-A)}{C - AD}\right] - 2} \quad (13)$$

Since I_o is always calculated at the point of (V_{oc},0) [2], so we have

$$I_o = \frac{D - \frac{V_{oc}}{A}}{\exp\left[\frac{V_{oc}}{C - AD}\right] - 2} \quad (14)$$

Finally, by replacing Eq. (14) in Eq. (9), the fifth parameter (I_L) can be computed from the following equation:

$$I_L = D - I_o \quad (15)$$

It can clearly be seen that, after determining A, B, C and D, the five parameters of solar cell are computed in sequence by using Eqs. (10), (11), (12), (14), and (15).

3. Determining the *I–V* and *P–V* curves of solar cell and module using a proposed feed-forward neural network

As mentioned, Eq. (3) represents the relation between the current (I) and the voltage ($V(I)$) of a solar cell. In this study, I and $V(I)$ are considered as the input and the output of a proposed feed-forward neural network, respectively. The proposed feed-forward neural network consists of six "Log-Sigmoid" hidden layers and one linear output layer. The transfer function of each hidden layer is considered as "Log-Sigmoid" because it is derived from Eq. (1) that $V(I)$ can approximately be expressed as a "Log-function" of I and furthermore, the output layer is chosen as linear in order to adjust the linear part of the Eq. (1). Since seven experimental data points have been used in [22–24], and for providing a comprehensive comparison and evaluation between the results of this study and other different methods presented in [22–24], only seven experimental data points are used for learning the proposed feed-forward neural network. Thus, to set the square error of the proposed neural network equal to zero, the minimum number of the neural network layers is seven so that each layer consists of only one neuron because there will be seven weights which have to be determined by learning the neural network (all biases of the seven layers are considered as unit). It can be summarized that six "Log-Sigmoid" hidden layers are chosen to adjust the nonlinear part of the Eq. (1) and one linear output layer is considered to adjust the linear part of the Eq. (1).

Consequently, the transfer functions of six hidden layers are "log $sig(x)$" while the transfer function of the output layer is "*purelin*(x)". The proposed feed-forward neural network is shown in Fig. 1. As mentioned before, all biases of the seven layers are considered as unit, so we have

$$b_1 = b_2 = b_3 = b_4 = b_5 = b_6 = b_7 = 1 \tag{16}$$

where b_k is the bias of the kth layer. By considering the structure of the proposed neural network, it can be found that

$$V(I) = purlin\{w_7 \cdot \log sig[w_6 \cdot \log sig(\ldots w_1 \cdot \log sig(I) + 1 \ldots) + 1] + 1\} \tag{17}$$

where $w_1, w_2, \ldots, w_6$ and w_7 are the weights of the first layer, second layer, ..., sixth layer and seventh layer, respectively.

Now, seven experimental data points are necessary to learn the proposed feed-forward neural network using the "Batch Learning-LMS algorithm". There is a similarity between the characteristics of solar cells and the step response of a first order system. Therefore, the seven distributed experimental data points on the curve, which are necessary for learning the proposed feed-forward neural network, can be selected as following:

$$I_0 = \frac{1}{4} I_{mp} \tan\theta_1 \tag{18}$$

$$I_1 = \frac{1}{2} I_{mp} \left[1 - \frac{1}{4}(1 - \cos\theta)\right] \tag{19}$$

$$I_2 = I_{mp} \left[1 - \frac{1}{4}(1 - \cos\theta)\right] \tag{20}$$

$$I_3 = I_{mp} \tag{21}$$

$$I_4 = I_{mp} + \frac{1}{4}(1 - \cos\theta)(I_{sc} - I_{mp}) \tag{22}$$

$$I_5 = \frac{1}{2}(I_{sc} + I_{mp}) + \frac{1}{8}(1 - \cos\theta)(I_{sc} - I_{mp}) \tag{23}$$

$$I_6 = I_{sc} \sin\theta_2 \tag{24}$$

These seven experimental data points and the angles θ, θ_1 and θ_2 are shown in Fig. 2.

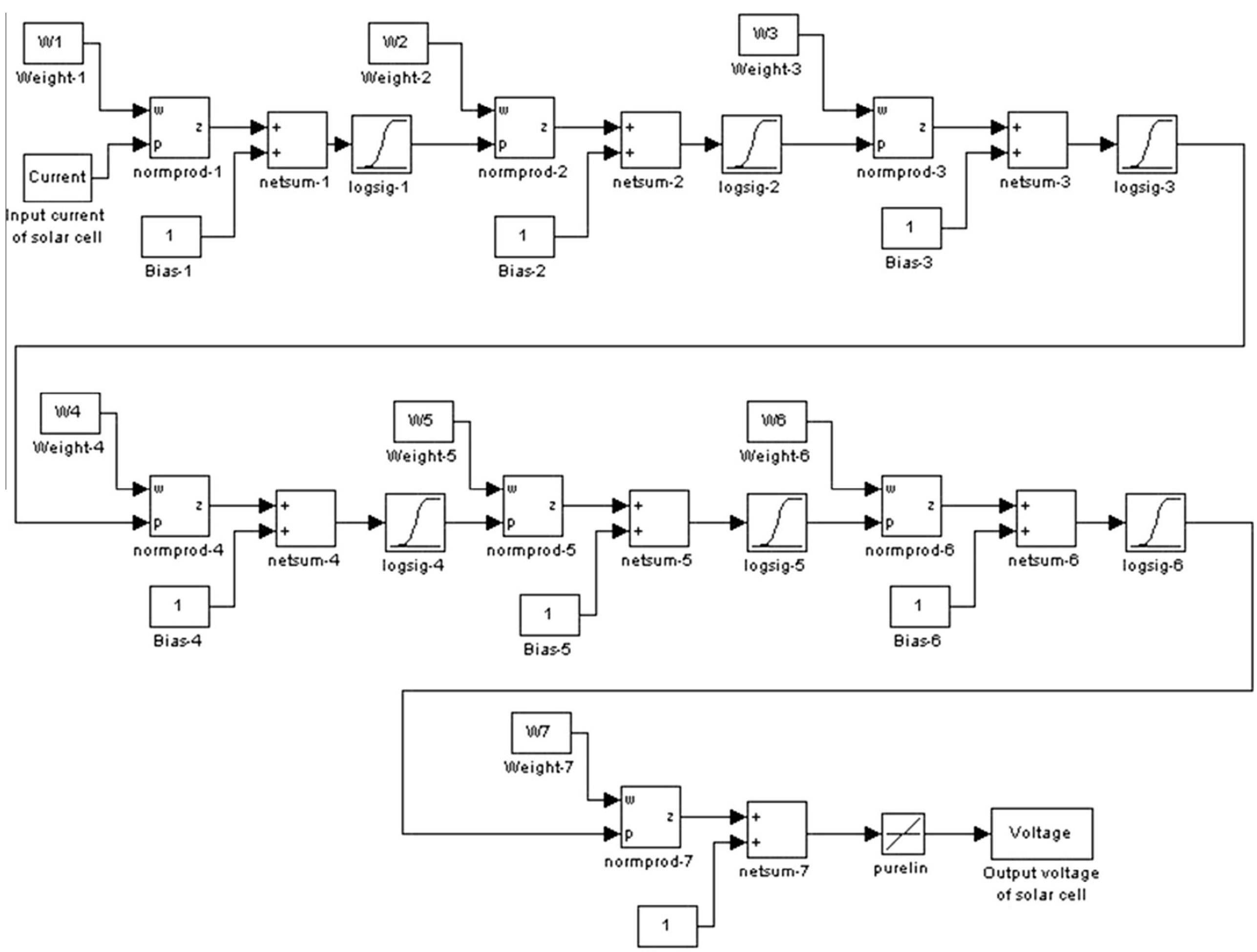

Fig. 1. The proposed feed-forward artificial neural network.

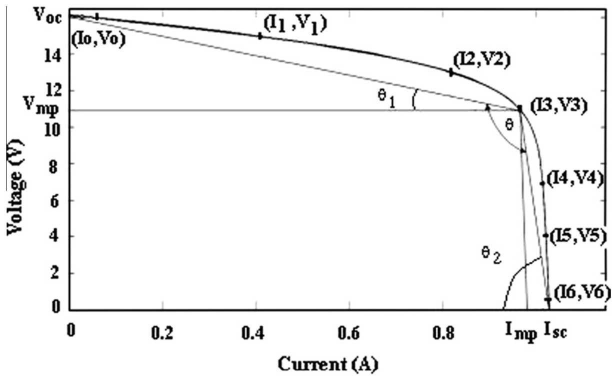

Fig. 2. The seven experimental data used for neural network learning.

The "Batch Learning-LMS algorithm" together with the above seven experimental data points is used to learn the proposed feed-forward neural network. After learning the proposed neural network, the layers weights of the network ($w_1, w_2, \ldots, w_6$ and w_7) are determined. Now, the *I–V* curve of the solar cell is calculated and simulated by varying the input of the learned neural network (current *I*) in the range of $(0, I_{sc})$ and measuring the output of the learned neural network (voltage $V(I)$). Similarly, the *P–V* curve of the solar cell is calculated and simulated by noting that for each point of the *P–V* curve we have $P = V \cdot I$.

Learning the proposed feed-forward neural network, calculating and simulating the *I–V* and *P–V* curves are again repeated for the silicon solar module and the plastic solar cell.

4. Simulation results

To prove the validity of the proposed method, the experimental data of a silicon solar cell and module reported by Easwarakhanthan in [25] was used. Furthermore, the experimental data of another type of solar cell presented in [20], which is called "plastic solar cell", was used too. The Refs. [20–24] are considered for comparing because they are the latest and the related works which have presented statistical results. Each reference reported only a portion of the research, for example Ref. [20] reported the results for the "plastic solar cell" while [21–23] reported the results for the "silicon solar cell and module". A report for both "plastic solar cell" and "silicon solar cell and module" is available in [24].

Learning the proposed feed-forward neural network for silicon solar cell, silicon solar module, plastic solar cell was carried out using the Neural Network Tool (NNTOOL) of Matlab software while all calculations and simulations were done in Matlab/Simulink environment.

The *I–V* and *P–V* curves of the silicon solar cell and silicon solar module, which were calculated and simulated using the proposed feed-forward neural network, together with the real experimental data are shown in Figs. 3(a)–4(b), respectively. For providing a comprehensive comparison and evaluation, the errors in this work and other different methods presented in [22–24] are shown in Figs. 5(a)–6(b). The figures show that the estimations of the *I–V* and *P–V* curves were accurately carried out using the proposed feed-forward neural network, so that the simulation results are

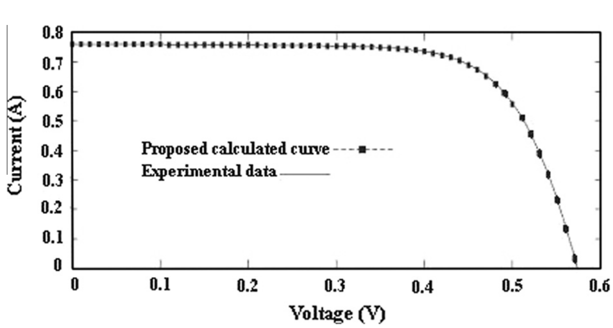

Fig. 3(a). Experimental data and calculated *I–V* curve for the silicon solar cell.

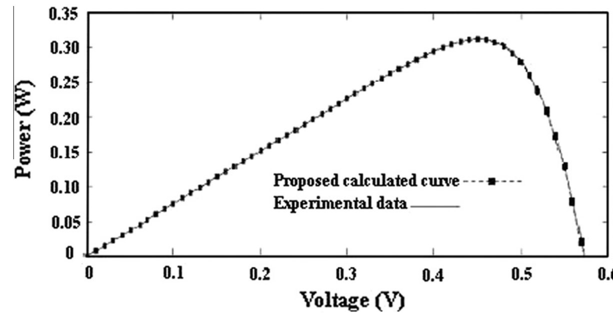

Fig. 3(b). Experimental data and calculated *P–V* curve for the silicon solar cell.

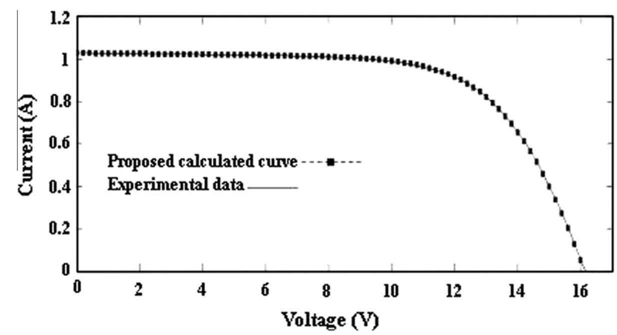

Fig. 4(a). Experimental data and calculated *I–V* curve for the silicon solar module.

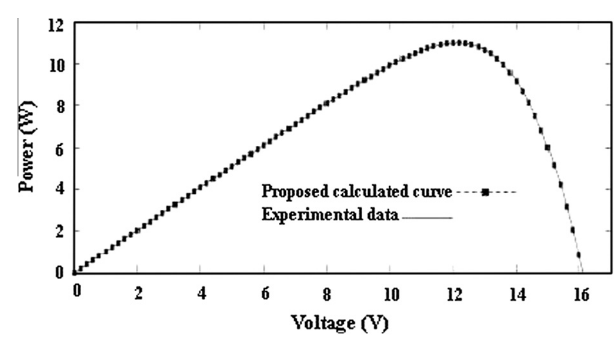

Fig. 4(b). Experimental data and calculated *P–V* curve for the silicon solar module.

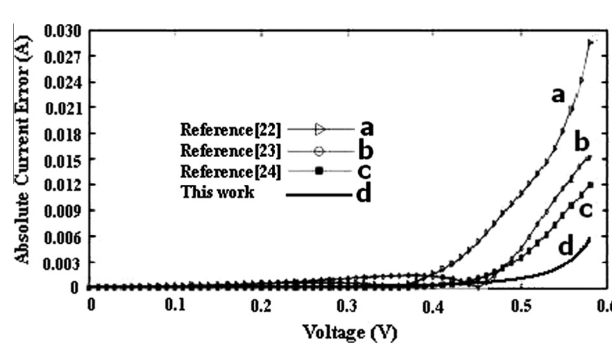

Fig. 5(a). Absolute current errors for the silicon solar cell.

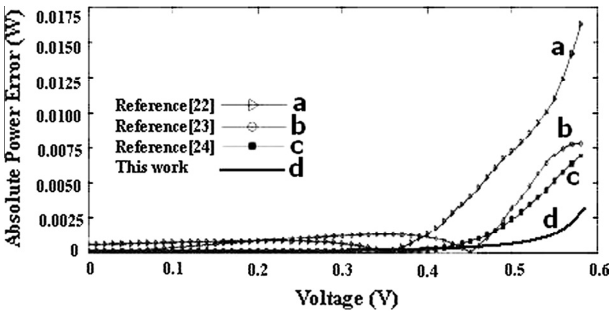

Fig. 5(b). Absolute power errors for the silicon solar cell.

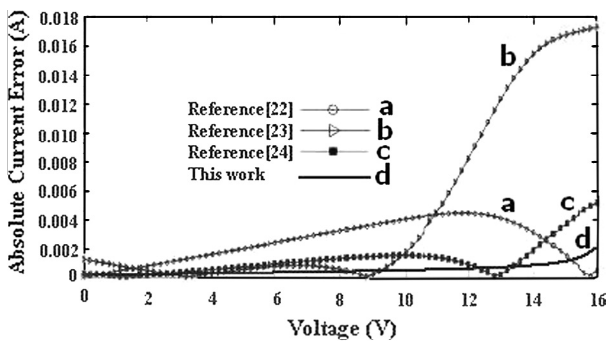

Fig. 6(a). Absolute current errors for the silicon solar module.

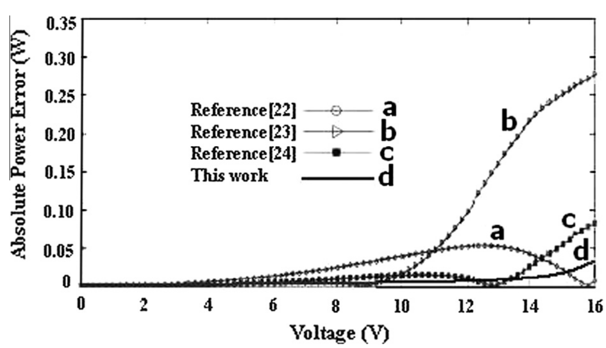

Fig. 6(b). Absolute power errors for the silicon solar module.

in good agreement with the experimental results. Comparison between the errors of the different methods shown in Figs. 5(a)–6(b) explicitly shows superiority of the proposed method to other methods. The *I–V* and *P–V* curves of the plastic solar cell calculated and simulated using the proposed method are also shown in

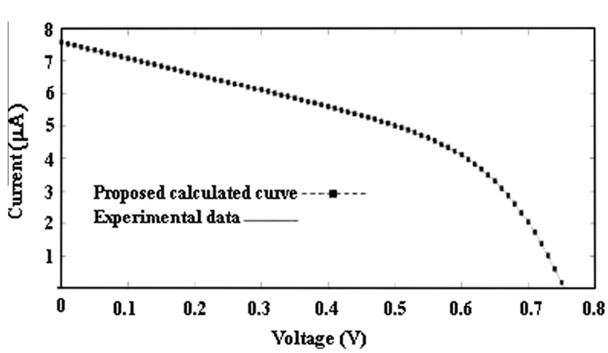

Fig. 7(a). Experimental data and calculated *I–V* curve for the plastic solar cell.

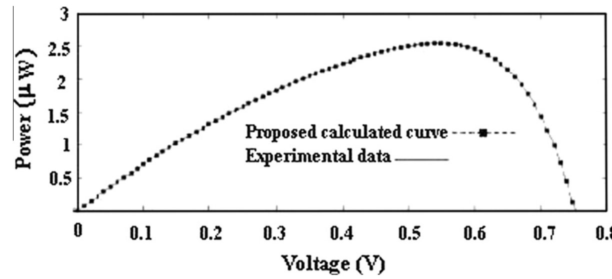

Fig. 7(b). Experimental data and calculated *P–V* curve for the plastic solar cell.

Figs. 7(a) and 7(b). The statistical results of this study for the silicon solar cell, silicon solar module and plastic solar cell together with the statistical results of other methods are presented in Tables 1–3, respectively. It can easily be seen that the proposed method current and power errors presented in Tables 1–3 are generally very lower than these errors in other methods especially at the MPP, defined as a point of the *I–V* curve at which the solar cell delivers the maximum output power. To obtain PV modules high performances the Maximum Power Point Tracking (MPPT) is a necessary strategy to adopt, it represents the subject of many researches in photovoltaic systems [28–30].

5. Calculation of the model parameters

The left side of Eq. (5) can be expressed as

$$S(V,I) = \int_0^I V(I)dI \approx \sum_{k=0}^{N} V(I_k)\cdot \Delta I = \Delta I \cdot \sum_{k=0}^{N} V(k\cdot \Delta I) \tag{25}$$

where $I = (N + 1)\Delta I$.

Replacing Eq. (25) in Eq. (5) results that

$$\Delta I \cdot \sum_{k=0}^{N} V(k\cdot\Delta I) \approx \frac{1}{2A}\left[[-V - B(N+1)\Delta I + C]^2 - (-V + C)^2\right] - \frac{1}{2}B[(N+1)\Delta I]^2 + AD(N+1)\Delta I \tag{26}$$

Previous studies have shown that R_s impacts on the *I–V* curve near the maximum power point while R_p determines the slope of the *I–V* curve between V_{oc} and V_{mp}. A typical approach [6] is to estimate R_s and R_p values by using the slopes at the V_{oc} and I_{sc}, respectively. The currents I_o and I_L are always calculated at the points of $(V_{oc},0)$ and $(0,I_{sc})$, respectively. Also, *n* is determined by the inherent characteristics of the solar cells [3]. Consequently, to accurately calculate the five parameters, the four different groups of the values of $S(V,I)$ are chosen at the experimental points I_0, I_2, I_4, and I_6 expressed by Eqs. (18), (20), (22), and (24), respectively [24]. By substituting these four groups of the values of $S(V,I)$ in Eq. (26), a set of equations consisting of four algebraic equations is generated. The *A*, *B*, *C* and *D* can be determined by solving these four algebraic equations.

The discrete form of the four experimental points I_0, I_2, I_4, and I_6 can be expressed as

$$I_0 = (N_0 + 1)\cdot \Delta I \tag{27}$$

Table 1
Statistical results for the silicon solar cell using different methods (33 °C).

Parameter	Ref. [23]	Ref. [22]	Ref. [24]	This work
CMAE (A)	0.01550	0.02819	0.01258	0.006
CMAEmp (A)	6.998×10^{-5}	7.934×10^{-3}	1.551×10^{-3}	7.231×10^{-4}
PMAE (W)	0.008834	0.01607	0.007174	0.003421
PMAEmp (W)	3.149×10^{-5}	3.570×10^{-3}	6.980×10^{-3}	3.253×10^{-4}

Table 2
Statistical results for the silicon solar module using different methods (45 °C).

Parameter	Ref. [23]	Ref. [22]	Ref. [24]	This work
CMAE (A)	0.01731	0.004423	0.005152	0.0021
CMAEmp (A)	0.0090	0.0043	0.0007	0.0009
PMAE (W)	0.2770	0.05394	0.08244	0.0336
PMAEmp (W)	0.1098	0.0535	0.0089	0.0114

Table 3
Statistical results for plastic solar cell using different methods (27.3 °C).

Parameter	Ref. [20]	Ref. [24]	This work
CMAE (μA)	920.93	1.33	0.42
CMAEmp (μA)	106.74	0.188	0.163
PMAE (μW)	841	0.999	0.3155
PMAEmp (μW)	59.775	0.106	0.092

Table 4
Parameters for the silicon solar cell using different methods (33 °C).

Parameter	Ref. [21]	Ref. [23]	Ref. [22]	Ref. [24]	This work
I_L (A)	0.7608	0.7603	0.7617	0.7609	0.7607
I_o (μA)	0.3223	0.3374	0.9980	0.3220	0.3231
n	1.4837	1.4841	1.6000	1.4837	1.4839
R_s (Ω)	0.0364	0.0376	0.0313	0.0364	0.0366
G_p (Ω^{-1})	0.0186	0.0094	0.0156	0.0185	0.0173

Table 5
Parameters for the silicon solar module using different methods (45 °C).

Parameter	Ref. [21]	Ref. [23]	Ref. [22]	Ref. [24]	This work
I_L (A)	1.0318	1.0300	1.0313	1.0313	1.0312
I_o (μA)	3.2876	6.3986	3.1756	3.2212	3.1822
n	48.4500	50.9900	48.2889	48.3221	48.2993
R_s (Ω)	1.2057	1.1619	1.2053	1.2132	1.2083
G_p (Ω^{-1})	0.0018	0.0014	0.0014	0.0016	0.0017

Table 6
Parameters of the plastic solar cell using different methods (27.3 °C).

Parameter	Ref. [20]	Ref. [24]	This work
I_L (A)	0.0079	0.0079	0.0079
I_o (μA)	0.0329	0.0136	0.0142
n	2.59	2.3101	2.3742
R_s (Ω)	8.586	8.5884	8.5873
G_p (Ω^{-1})	0.0050	0.0051	0.0052

$$I_2 = (N_2 + 1) \cdot \Delta I \tag{28}$$

$$I_4 = (N_4 + 1) \cdot \Delta I \tag{29}$$

$$I_6 = (N_6 + 1) \cdot \Delta I \tag{30}$$

Substituting $\Delta I = 0.0001$ [A] and the four experimental points $I_0 = 0.1$ [A], $I_2 = 0.6$ [A], $I_4 = 0.7$ [A], $I_6 = 0.75$ [A] in Eqs. (27)–(30) results that $N_0 = 999$, $N_2 = 5999$, $N_4 = 6999$, $N_6 = 7499$. By replacing $N_0 = 999$, $N_2 = 5999$, $N_4 = 6999$, and $N_6 = 7499$ together with $\Delta I = 0.0001$ [A] and $V(k \cdot \Delta I)$, which were calculated to determine the I–V curve in previous section using the learned feed-forward neural network, in Eq. (26), we have four algebraic equations that A, B, C and D are determined by solving these four algebraic equations. Then, the five parameters of the solar cell (G_p,R_s,n,I_o,I_L) are computed in sequence by substituting A, B, C and D, into Eqs. (10), (11), (12), (14), and (15).

To make a comparison between the different methods, the five parameters (G_p,R_s,n,I_o,I_L) of silicon solar cell, silicon solar module and plastic solar cell calculated using the proposed method and other methods are presented in Tables 4–6, respectively. It can be seen that the five parameters extracted using the proposed method, are very close to those reported in the other references.

6. Conclusion

A new method based on using neural network and Lambert W function was proposed. Determining the I–V and P–V characteristics of a silicon solar cell, a silicon solar module and a plastic solar cell were accurately carried out using the proposed technique. Simulation results proved that the model parameters and the estimated I–V and P–V characteristics using the proposed method have higher accuracy than that in other methods. Furthermore, the estimated model parameters and characteristics are in good agreement with the real experimental results. The simulation results also showed that the current and power errors in the proposed method are generally very lower than other methods error even at the MPP.

References

[1] Pujol L, Perona A, Bouriel JR, Landart E, Dollet A. Outdoor characterization and performance evaluation of integra-sun prototype CPV module. In: Proc 6th int conf. on concentrating photovoltaic systems, vol. 1277; 2010. p. 179–82.
[2] Law DC, King RR, Yoon H, Archer MJ, Boca A, Fetzer CM, et al. Future technology pathways of terrestrial III–V multijunction solar cells for concentrator photovoltaic systems. J Solar Energy Mater Solar Cells 2010;94:1314–8.
[3] De Soto W, Klein SA, Beckman WA. Improvement and validation of a model for photovoltaic array performance. J Solar Energy 2006;80:78–88.
[4] Carrero C, Rodrıguez J, Ramrez D, Platero C. Simple estimation of PV modules loss resistances for low error modelling. J Renew Energy 2010;35:1103–8.
[5] Brano VL, Orioli A, Ciulla G, Gangi AD. An improved five-parameter model for photovoltaic modules. J Solar Energy Mater Solar Cells 2010;94:1358–70.
[6] Chouder A, Silvestre S, Sadaoui N, Rahmani L. Modeling and simulation of a grid connected PV system based on the evaluation of main PV module parameters. J Simul Model Practice Theor 2012;20:46–58.
[7] Karatepe E, Boztepe M, Colak M. Development of a suitable model for characterizing photovoltaic arrays with shaded solar cells. J Solar Energy 2007;81:977–92.
[8] Chen Y, Wang X, Li D, Hong R, Shen H. Parameters extraction from commercial solar cells I–V characteristics and shunt analysis. J Appl Energy 2011;88:2239–44.
[9] Xiao W, Lind MGJ, Dunford WG, Capel A. Real-time identification of optimal operating points in photovoltaic power systems. IEEE Trans Ind Electron 2006;53:1017–26.
[10] Abebe H, Cumberbatch E, Morris H, Tyree V, Numata T, Uno S. Symmetric and asymmetric double gate MOSFET modeling. J Semicond Technol Sci 2009;9:225–32.
[11] Jain A, Kapoor A. Exact analytical solutions of the parameters of real solar cells using Lambert W-function. J Solar Energy Mater Solar Cells 2004;81:269–77.
[12] Jain A, Kapoor A. Exact analytical solutions of the parameters of real solar cells using Lambert W-function. J Solar Energy Mater Solar Cells 2005;85:391–6.
[13] Singh NS, Jain A, Kapoor A. Determination of the solar cell junction ideality factor using special trans function theory (STFT). J Solar Energy Mater Solar Cells 2009;93:1423–6.
[14] Ortiz-Conde A, Sanchez FJG, Muci J. New method to extract the model parameters of solar cells from the explicit analytic solutions of their illuminated I–V characteristics. Solar Energy Mater Solar Cells 2006;90:352–61.
[15] Corless RM, Gonnet GH, Hare DEG, Jeffrey DJ, Knuth DE. On the Lambert W function. Adv Computat Math 1996;5:329–59.
[16] Veberic D. Lambert W function for applications in physics. J Comput Phys Commun 2012;183:2622–8.
[17] Zagrouba M, Sellami A, Bouaıcha M, Ksouri M. Identification of PV solar cells and modules parameters using the genetic algorithms: application to maximum power extraction. J Solar Energy 2010;84:860–6.
[18] AlHajri MF, El-Naggar KM, AlRashidi MR, Al-Othman AK. Optimal extraction of solar cell parameters using pattern search. J Renew Energy 2012;44:238–45.
[19] Ye M, Wang X, Xu Y. Parameter extraction of solar cells using particle swarm optimization. J Appl Phys 2009;105:94501–7.
[20] Chegaar M, Azzouzi G, Mialhe P. Simple parameter extraction method for illuminated solar cells. J Solid-State Electron 2006;50:1234–7.

[21] AlRashidi MR, AlHajri MF, El-Naggar KM, Al-Othman AK. A new estimation approach for determining the *I–V* characteristics of solar cells. J Solar Energy 2011;85:1543–50.
[22] Ishaque K, Salam Z. An improved modeling method to determine the model parameters of photovoltaic (PV) modules using differential evolution (DE). J Solar Energy 2011;85:2349–59.
[23] Ding J, Radhakrishnan R. A new method to determine the optimum load of a real solar cell using the Lambert W-function. J Solar Energy Mater Solar Cells 2008;92:1566–9.
[24] Peng L, Sun Y, Meng Z, Wang Y, Xu Y. A new method for determining the characteristics of solar cells. J Power Sources 2013;227:131–6.
[25] Easwarakhanthan T, Bottin J, Bouhouch I, Boutrit C. Nonlinear minimization algorithm for determining the solar cell parameters with microcomputers. J Solar Energy 1986;4:1–12.
[26] Amrouche B, Guessoum A, Belhamel M. A simple behavioural model for solar module electric characteristics based on the first order system step response for MPPT study and comparison. J Appl Energy 2012;91:395–404.
[27] Ismail MS, Moghavvemi M, Mahlia TMI. Characterization of PV panel and global optimization of its model parameters using genetic algorithm. J Energy Convers Manage 2013;73:10–25.
[28] Tsang KM, Chan WL. Model based rapid maximum power point tracking for photovoltaic systems. J Energy Convers Manage 2013;70:83–9.
[29] Tsang KM, Chan WL. Three-level grid-connected photovoltaic inverter with maximum power point tracking. J Energy Convers Manage 2013;65:221–7.
[30] Ammar Majed Ben, Chaabene Maher, Chtourou Zied. Artificial neural network based control for PV/T panel to track optimum thermal and electrical power. J Energy Convers Manage 2013;65:372–80.